

Computation of Oscillation Frequency in a Plasma Filled Rectangular Cavity Resonator

Pragya Shilpi*, Dharmendra Upadhyay, and Harish Parthasarathy

Abstract—Oscillation frequency in a plasma filled rectangular dielectric resonator antenna is computed. Perturbation method for solving differential equation is applied to find oscillation frequencies of dielectric cavity resonator. Equilibrium distribution function of collisionless Boltzmann equation is slightly perturbed. Distribution function of plasma is perturbed by altering external applied electromagnetic field. Perturbed Boltzmann equation satisfies with the relaxation time approximation used for the collision. The resulting Maxwell equations are subjected to appropriate boundary condition. Multilinear algebra tensor decomposition technique is done to find eigenfrequencies of cavity resonator antenna considered in this paper. A simulation study of a ionized gas plasma antenna is done on HFSS. Numerically calculated oscillation frequency is cross verified with HFSS result and found in good agreement.

1. INTRODUCTION

Maxwell's equations can be solved either in time domain or in frequency domain. By assuming harmonics $\exp(j\omega t)$, we find the response of a driving system such as its eigenvalues. Eigenvalues are the natural oscillation frequencies of the system. To model the source of excitation of a given system "Green's function" is of utmost importance. As we write impulse response function for circuit, Green's function plays the same role in electromagnetism. By definition it gives response of an electromagnetic system to delta source, which is an important analytical tool for procuring the response of any arbitrary system by the method of superposition. In this paper, our aim to construct a Green's function for plasma and find the eigenfrequencies of a plasma filled cavity resonator.

In this manuscript, we start with equilibrium state of distribution function of plasma. The equilibrium distribution function is the time independent solution of the Boltzmann equation in the absence of external force. In equilibrium state, there is no spatial gradient of particle number density, and the interaction or collision between particles does not change distribution function. Collisionless Boltzmann equation is give by

$$d^6 N_\alpha(\mathbf{r}, \mathbf{v}, t) = f_\alpha(\mathbf{r}, \mathbf{v}, t) d^3 r d^3 v$$

Above mentioned equation represents the number of particles of type α , enclosed within the volume element at an instant t . According to Boltzmann equation, the equilibrium distribution function satisfies the following condition

$$\left(\frac{\delta f}{\delta t} \right)_{coll} = 0$$

To account for the collision "relaxation model" of plasma is considered. It is assumed that the effect of collision is to restore the situation of local equilibrium. Local equilibrium is characterized by the

Received 12 November 2020, Accepted 7 January 2021, Scheduled 15 January 2021

* Corresponding author: Pragya Shilpi (pragya.shilpi4@gmail.com).

The authors are with the Netaji Subhas Institute of Technology, New Delhi, India.

distribution function $f_{\alpha 0}(\mathbf{r}, \mathbf{v})$. It is assumed that initially the situation is not in equilibrium in the absence of external force, described by distribution function $f_{\alpha}(\mathbf{r}, \mathbf{v}, t)$ different from $f_{\alpha 0}(\mathbf{r}, \mathbf{v})$. After collision situation reaches a local equilibrium condition exponentially with time having a relaxation time τ . Relaxation time is in the order of time between two consecutive collisions. and is written as ν^{-1} , where ν represents a collision frequency. This model was developed by Krook and mathematically represented as

$$\left(\frac{\delta f}{\delta t}\right)_{coll} = -\frac{f_{\alpha} - f_{\alpha 0}}{\tau}$$

The solution of above differential equation is given by

$$f_{\alpha}(\mathbf{v}, t) = f_{\alpha 0} - [f_{\alpha}(\mathbf{v}, t) - f_{\alpha 0}]e^{-t/\tau}$$

A pragmatic way to describe the dynamics of plasma is to consider that the plasma particle motion is governed by the applied external fields plus macroscopic internal electromagnetic fields. Boltzmann equation is given by

$$\frac{\partial f(\mathbf{r}, \mathbf{v}, t)}{\partial t} + \mathbf{v} \cdot \nabla f(\mathbf{r}, \mathbf{v}, t) + \mathbf{a} \cdot \nabla_{\mathbf{v}} f(\mathbf{r}, \mathbf{v}, t)$$

with the collision term $(\delta f_{\alpha}/\delta t)_{coll}$ equal to zero, including the external force and internal fields. We turn up to a partial differential equation that describes the time evolution of the distribution function in the phase space (six dimensional space given as $d^3r d^3v$) known as Vlasov equation.

$$\frac{\partial f_{\alpha}}{\partial t} + \mathbf{v} \cdot \nabla f_{\alpha} + \frac{1}{m_{\alpha}} [\mathbf{F}_{\text{ext}} + q_{\alpha}(\mathbf{E}_{\mathbf{i}} + \mathbf{v} \times \mathbf{B}_{\mathbf{i}})] \cdot \nabla f_{\alpha} = 0$$

Time-domain analysis of the forced oscillations in a cavity filled with a plasma in which the system of time derivative Maxwell's equations and the time derivative motion equation for the plasma is solved simultaneously in [1]. Resonating modes inside cavity give insight into antenna design, impedance, and radiation patterns which is covered in [2]. And discussion of how higher-order modes generated and control impact bandwidth and antenna gain is also done. The simulation data of the spatial distributions of the electron energy density and concentrations of electrons of argon plasma filled in Beenakker cavity are examined in [3]. Analysis of the effect of the background plasma on the electromagnetic properties of coaxial resonators leading to a decrease or an increase in the resonance frequencies is shown in [4]. For a dispersive non-magnetized collisional plasma medium, wave propagation is modeled by finite difference time domain method [5]. A resonator cavity filled with plasma is utilized as a microwave plasma lamp with a different light emitting mechanism [6]. Relaxation time of plasma is calculated by gauge theory or string theory in [7]. Probe diagnostic is used to find plasma parameters [8]. Kinetic theory of plasma is illustrated by Vlasov equations. Vlasov equation is equivalent equation as Boltzmann distribution function which account for wave-particle and particle-particle interaction [9]. Kinetic theory of plasma is studied to acquire partial distribution function. To account for all microscopic details of plasma (such as collisions among plasma particles), a kinetic model is given [10]. The dispersion relation for a open cavity filled with plasma grating is studied. Under a strong wave modulation, plasma forms a periodical density grating leading to periodical perturbation in dielectric constant of cavity medium [11]. Relaxation time in the plasma is derived, which shows that it is dependent on the time taken by the shock wave to pass through the discharge tube. The authors show that the speed of shock wave is only a function of circuit inductance and capacitance and is independent of other discharge parameters [12]. The shift in resonance frequency is calculated by applying electromagnetic boundary conditions to dispersion relation. A cylindrical cavity partially filled with plasma having constant longitudinal magnetic field is analyzed, and its natural frequencies are numerically calculated [13].

The dispersion relation is obtained for hybrid modes in a plasma waveguide filled with dielectric having cylindrical metallic wall with an elliptic cross section. The plasma region is placed on the outer surface of a dielectric tube of waveguide which is analyzed in [14]. Relaxation time estimation in non-ideal dusty plasma and characteristic relaxation times of vertical and horizontal motions of dust particles in gas discharge are calculated by analytical approach, and the analysis of simulation results is done in [15]. Magnetic field changes the plasma to anisotropic media, and its field analysis in a coaxial gyrotron cavity with triangular corrugations is done in [16]. The plasma in coaxial cavity with wedge-shaped corrugations on and inside the gyrotron cavity is a perfect vacuum which is tackled in [17].

A comprehensive analysis of fundamentals of plasma environment utilizing statistical kinetic theory is covered in book [18]. The motion of plasma particles under the application of force is formulated, and the concept of phase space and distribution function is also considered. In book [19], the analysis and design of several types antennas are given. In book [20], Raman scattering, resonance absorption, and stimulated Brillouin in plasma are examined. Spontaneous and magnetic field generation in plasma along with inertial confinement fusion is carried out.

In [21], an argon plasma antenna is designed whose gas composition and pressure of gas could be customized. In [22], a large gyrotron is realized for different operating magnetic fields, and resultant harmonics are measured. A theoretical analysis of Green's function methods applied to quantum systems under equilibrium and without equilibrium for single molecule junctions is given in [23].

2. RESEARCH HIGHLIGHTS

The plasma within the cavity is perturbed by an EM field. Likewise, the EM field within the cavity gets perturbed by charge and current density given by the plasma distribution. When we apply perturbation theory to the problem, the plasma distribution function is perturbed as we perturb the electromagnetic field. To satisfy a set of linearized equations it is better to approximate boundary partial differential equation condition. The boundary condition is applied on the side wall of plasma filled cavity. Distribution function and electro magnetic equation determine the possible set of eigenfunctions of oscillation by a appropriate design of the cavity. The equations can determine these oscillator eigenfrequencies. By controlling the permittivity, one or more of the characteristic oscillation frequency matches the channel resonant frequency, over which we can transmit the waves from the plasmonic antenna.

3. FORMULATIONS AND EQUATIONS

Equilibrium distribution function of plasma is described as

$$f_0(\mathbf{r}, \mathbf{v}) = C \cdot \exp\left(-\beta m \left(\frac{v^2}{2} + U(\mathbf{r})\right)\right) \quad (1)$$

And perturbed plasma distribution is given by

$$f(t, \mathbf{r}, \mathbf{v}) = f_0(\mathbf{r}, \mathbf{v}) + f_1(t, \mathbf{r}, \mathbf{v}) \quad (2)$$

f_0 satisfies equilibrium collisionless Boltzmann equation.

$$(\mathbf{v}, \nabla_r) f_0 - (\nabla U(\mathbf{r}), \nabla_v) f_0 = 0 \quad (3)$$

f_1 satisfies the perturbed Boltzmann equation with the relaxation time approximation used for the collision.

$$\frac{\partial f_1}{\partial t} + (\mathbf{v}, \nabla_r) f_1 + \frac{q}{m} (\mathbf{E}(t, \mathbf{r}) + \mathbf{v} \times \mathbf{B}(t, \mathbf{r}), \nabla_v) f_0(\mathbf{r}, \mathbf{v}) + \frac{f_1(t, \mathbf{r}, \mathbf{v})}{\tau} = 0 \quad (4)$$

or

$$\frac{\partial f_1}{\partial t} + (\mathbf{v}, \nabla_r) f_1 + \frac{q}{m} (\mathbf{E}, -\beta m \mathbf{v}) f_0 + \frac{f_1}{\tau} = 0$$

or

$$\frac{\partial f_1}{\partial t} + (\mathbf{v}, \nabla_r) f_1 - \beta q (\mathbf{E}, \mathbf{v}) f_0 + \frac{f_1}{\tau} = 0$$

Charge density within the guide

$$\rho(t, \mathbf{r}) = q \int f_1(t, \mathbf{r}, \mathbf{v}) d^3 v \quad (5)$$

Current density within the guide

$$\mathbf{J} = (t, \mathbf{r}) = q \int \mathbf{v} f_1(t, \mathbf{r}, \mathbf{v}) d^3 v \quad (6)$$

Maxwell's equations are

$$\nabla \times \mathbf{E} = -\frac{\partial \mathbf{B}}{\partial t} \quad (7a)$$

$$\nabla \times \mathbf{B} = \mu \mathbf{J} + \mu \epsilon \frac{\partial \mathbf{E}}{\partial t} \quad (7b)$$

$$\nabla \cdot \mathbf{E} = \frac{\rho}{\epsilon} \quad (7c)$$

$$\nabla \cdot \mathbf{B} = 0 \quad (7d)$$

Combining the curl equations

$$\begin{aligned} \nabla(\nabla \cdot \mathbf{E}) - \nabla^2 \mathbf{E} &= -\frac{\partial}{\partial t} \left(\mu \mathbf{J} + \mu \epsilon \frac{\partial \mathbf{E}}{\partial t} \right) \\ \nabla^2 \mathbf{E} - \mu \epsilon \mathbf{E}_{,tt} &= \mu \mathbf{J}_{,t} + \frac{\nabla \rho}{\epsilon} \end{aligned} \quad (8)$$

Resonator has perfect conducting walls. $E_z = 0$ at $X = 0, a$ and $Y = 0, b$. $E_X = 0$ at $Y = 0, b$ and $z = 0, d$. $E_Y = 0$ at $X = 0, a$ and $z = 0, d$.

Expanding in accordance with the boundary condition,

$$E_X(X, Y, z, t) = \sum_{mnp} E_X[nmpt] \cos\left(\frac{n\pi X}{a}\right) \sin\left(\frac{m\pi Y}{b}\right) \sin\left(\frac{p\pi z}{d}\right) \quad (9a)$$

$$E_Y(X, Y, z, t) = \sum_{mnp} E_X[nmpt] \sin\left(\frac{n\pi X}{a}\right) \cos\left(\frac{m\pi Y}{b}\right) \sin\left(\frac{p\pi z}{d}\right) \quad (9b)$$

$$E_z(X, Y, z, t) = \sum_{mnp} E_X[nmpt] \sin\left(\frac{n\pi X}{a}\right) \sin\left(\frac{m\pi Y}{b}\right) \cos\left(\frac{p\pi z}{d}\right) \quad (9c)$$

In the frequency domain $k^2 = \omega^2 \mu \epsilon$. We can write Equation (8) as

$$(\nabla^2 + k^2)\mathbf{E}(X, Y, z, \omega) = j\omega \mu \mathbf{J}(X, Y, z, \omega) + \frac{\nabla \rho(X, Y, z, \omega)}{\epsilon} = j\omega \mu \mathbf{J}(\mathbf{r}, \omega) + \frac{\nabla \rho(\mathbf{r}, \omega)}{\epsilon} \quad (10)$$

Expand X, Y, z components of the source field \mathbf{S} in a compatible manner and the e_{th} components of \mathbf{E} according to the boundary condition.

$$\mathbf{J}(\mathbf{r}, \omega) = q \int \mathbf{v} f_1(\omega, \mathbf{r}, \mathbf{v}) d^3 v \quad (11)$$

$$\nabla \rho(\mathbf{r}, \omega) = q \int \nabla f_1(\omega, \mathbf{r}, \mathbf{v}) d^3 v \quad (12)$$

$$\mathbf{S}(\mathbf{r}, \omega) = j\omega \mu \mathbf{J}(\mathbf{r}, \omega) + \frac{\nabla \rho(\mathbf{r}, \omega)}{\epsilon} \quad (13)$$

Expand the source field in terms of modal coefficient.

$$\begin{aligned} S_X(\mathbf{r}, \omega) &= \sum_{mnp} S_X[nmp, \omega] \cos\left(\frac{n\pi X}{a}\right) \sin\left(\frac{m\pi Y}{b}\right) \sin\left(\frac{p\pi z}{d}\right) \\ &= j\omega \mu q \int v_X \sum_{mnp} f_X[mnp, \omega, \mathbf{v}] \cos\left(\frac{n\pi X}{a}\right) \sin\left(\frac{m\pi Y}{b}\right) \sin\left(\frac{p\pi z}{d}\right) d^3 v \\ &\quad + \frac{q}{\epsilon} \int \sum_{mnp} \tilde{f}_X[mnp, \omega, \mathbf{v}] \cos\left(\frac{n\pi X}{a}\right) \sin\left(\frac{m\pi Y}{b}\right) \sin\left(\frac{p\pi z}{d}\right) d^3 v \end{aligned} \quad (14)$$

We expand distribution function in terms of modal basis function.

$$f_X[mnp, \omega, \mathbf{v}] = \frac{2\sqrt{2}}{\sqrt{abd}} \int v_X f_1(\omega, \mathbf{r}, \mathbf{v}) \cos\left(\frac{n\pi X}{a}\right) \sin\left(\frac{m\pi Y}{b}\right) \sin\left(\frac{p\pi z}{d}\right) d^3 v \quad (15)$$

Differentiating f_X w.r.t X ,

$$\tilde{f}_X[mnp, \omega, \mathbf{v}] = \left(\frac{-n\pi}{a}\right) \left(\frac{2\sqrt{2}}{\sqrt{abd}}\right)^2 \int f_1(\omega, \mathbf{r}, \mathbf{v}) \sin\left(\frac{n\pi X}{a}\right) \sin\left(\frac{m\pi Y}{b}\right) \sin\left(\frac{p\pi z}{d}\right) dX dY dz d^3v \quad (16)$$

Let

$$\begin{aligned} & j\omega\mu q \left(\frac{2\sqrt{2}}{\sqrt{abd}}\right)^2 \sum_{mnp=1}^N \cos\left(\frac{n\pi X}{a}\right) \sin\left(\frac{m\pi Y}{b}\right) \sin\left(\frac{p\pi z}{d}\right) \cos\left(\frac{n\pi X'}{a}\right) \sin\left(\frac{m\pi Y'}{b}\right) \sin\left(\frac{p\pi z'}{d}\right) \\ & = j\omega\mathcal{K}_X[X, Y, z|X', Y', z'] = j\omega\mathcal{K}_X[\mathbf{r}|\mathbf{r}'] \\ & \left(\frac{2\sqrt{2}}{\sqrt{abd}}\right)^2 \sum_{mnp=1}^N \left(\frac{-n\pi}{a}\right) \cos\left(\frac{n\pi X}{a}\right) \sin\left(\frac{m\pi Y}{b}\right) \sin\left(\frac{p\pi z}{d}\right) \sin\left(\frac{n\pi X'}{a}\right) \sin\left(\frac{m\pi Y'}{b}\right) \sin\left(\frac{p\pi z'}{d}\right) \\ & = \tilde{\mathcal{K}}_X[X, Y, z|X', Y', z'] = \tilde{\mathcal{K}}_X[\mathbf{r}|\mathbf{r}'] \end{aligned} \quad (17)$$

Then substitute RHS of Equation (17) into Equation (14).

$$S_X(\mathbf{r}, \omega) = j\omega \int \mathcal{K}_X[\mathbf{r}|\mathbf{r}'] v_X f_1(\omega, \mathbf{r}', \mathbf{v}) d^3r' d^3v + \int \tilde{\mathcal{K}}_X[\mathbf{r}|\mathbf{r}'] f_1(\omega, \mathbf{r}', \mathbf{v}) d^3r' d^3v \quad (18)$$

$$S_X(\mathbf{r}, \omega) = (\nabla^2 + k^2) E_X(\mathbf{r}, \omega)$$

$$E_X(\mathbf{r}, \omega) = \sum_{mnp} E_X[mnp, \omega] \cos\left(\frac{n\pi X}{a}\right) \sin\left(\frac{m\pi Y}{b}\right) \sin\left(\frac{p\pi z}{d}\right) \quad (19)$$

$$E_X[mnp, \omega] = \frac{S_X[mnp, \omega]}{\left(k^2 - \left(\frac{n^2}{a^2} + \frac{m^2}{b^2} + \frac{p^2}{d^2}\right) \pi^2\right)}$$

$$S_X[mnp, \omega] = j\omega\mu q \int v_X f_X[mnp, \omega, \mathbf{v}] d^3v + \frac{q}{\epsilon} \int \tilde{f}_X[mnp, \omega, \mathbf{v}] d^3v$$

Substitute the value of $S_X[mnp, \omega]$ into Equation (19).

$$\begin{aligned} E_X(\mathbf{r}, \omega) &= \sum_{mnp} \frac{j\omega\mu q \int v_X f_X[mnp, \omega, \mathbf{v}] d^3v + \frac{q}{\epsilon} \int \tilde{f}_X[mnp, \omega, \mathbf{v}] d^3v}{\left(k^2 - \left(\frac{n^2}{a^2} + \frac{m^2}{b^2} + \frac{p^2}{d^2}\right) \pi^2\right)} \cos\left(\frac{n\pi X}{a}\right) \sin\left(\frac{m\pi Y}{b}\right) \sin\left(\frac{p\pi z}{d}\right) \\ &= \sum_{mnp} \frac{\left(\frac{j\omega\mu q 2\sqrt{2}}{\sqrt{abd}} \int v_X f_1[\omega, \mathbf{r}', \mathbf{v}] \cos\left(\frac{n\pi X'}{a}\right) \sin\left(\frac{m\pi Y'}{b}\right) \sin\left(\frac{p\pi z'}{d}\right) \right)}{\cos\left(\frac{n\pi X}{a}\right) \sin\left(\frac{m\pi Y}{b}\right) \sin\left(\frac{p\pi z}{d}\right) dX' dY' dz' d^3v} \\ & \quad \left(k^2 - \left(\frac{n^2}{a^2} + \frac{m^2}{b^2} + \frac{p^2}{d^2}\right) \pi^2\right) \\ & + \sum_{mnp} \frac{\left(\frac{-n\pi q 2\sqrt{2}}{a\epsilon\sqrt{abd}} \int f_1[\omega, \mathbf{r}', \mathbf{v}] \sin\left(\frac{n\pi X'}{a}\right) \sin\left(\frac{m\pi Y'}{b}\right) \sin\left(\frac{p\pi z'}{d}\right) \right)}{\cos\left(\frac{n\pi X}{a}\right) \sin\left(\frac{m\pi Y}{b}\right) \sin\left(\frac{p\pi z}{d}\right) dX' dY' dz' d^3v} \\ & \quad \left(k^2 - \left(\frac{n^2}{a^2} + \frac{m^2}{b^2} + \frac{p^2}{d^2}\right) \pi^2\right) \end{aligned} \quad (20)$$

Let

$$L_X^{(1)}(\mathbf{r}|\mathbf{r}') = \sum_{mnp=1}^N \frac{\frac{\mu q (2\sqrt{2})^2}{abd} \cos\left(\frac{n\pi X'}{a}\right) \sin\left(\frac{m\pi Y'}{b}\right) \sin\left(\frac{p\pi z'}{d}\right) \cos\left(\frac{n\pi X}{a}\right) \sin\left(\frac{m\pi Y}{b}\right) \sin\left(\frac{p\pi z}{d}\right)}{\left(k^2 - \left(\frac{n^2}{a^2} + \frac{m^2}{b^2} + \frac{p^2}{d^2}\right) \pi^2\right)} \quad (21)$$

$$L_X^{(2)}(\mathbf{r}|\mathbf{r}') = \sum_{mnp=1}^N \frac{\frac{-n\pi q (2\sqrt{2})^2}{a\epsilon abd} \sin\left(\frac{n\pi X'}{a}\right) \sin\left(\frac{m\pi Y'}{b}\right) \sin\left(\frac{p\pi z'}{d}\right) \cos\left(\frac{n\pi X}{a}\right) \sin\left(\frac{m\pi Y}{b}\right) \sin\left(\frac{p\pi z}{d}\right)}{\left(k^2 - \left(\frac{n^2}{a^2} + \frac{m^2}{b^2} + \frac{p^2}{d^2}\right) \pi^2\right)} \quad (22)$$

Hence Equation (19) can be written as

$$E_X(\mathbf{r}, \omega) = j\omega \int L_X^{(1)}(\mathbf{r}|\mathbf{r}') v_X f_X[\omega, \mathbf{r}, \mathbf{v}] d^3 r' d^3 v + \int L_X^{(2)}(\mathbf{r}|\mathbf{r}') f_1[\omega, \mathbf{r}, \mathbf{v}] d^3 r' d^3 v \quad (23)$$

Likewise

$$(\nabla^2 + k^2)E_Y = S_Y(\mathbf{r}, \omega)$$

$$S_Y(\mathbf{r}, \omega) = j\omega\mu J_Y(\mathbf{r}, \omega) + \frac{\rho_{,Y}(\mathbf{r}, \omega)}{\epsilon} = j\omega\mu q \int v_Y f_1[\omega, \mathbf{r}, \mathbf{v}] d^3 v + \frac{q}{\epsilon} \int f_{1,Y}[\omega, \mathbf{r}, \mathbf{v}] d^3 v$$

where $\rho_{,Y}$ means differentiating ρ w.r.t Y , and $f_{1,Y}$ is the differentiation of f_1 w.r.t Y .

In accordance with the boundary condition on E_Y , we expand by using the basis function $\sin\left(\frac{n\pi X}{a}\right) \cos\left(\frac{m\pi Y}{b}\right) \sin\left(\frac{p\pi z}{d}\right)$.

Then we can write

$$\begin{aligned} & \mu q \int v_Y f_1[\omega, \mathbf{r}, \mathbf{v}] d^3 v \\ & \simeq \left(\frac{2\sqrt{2}}{\sqrt{abd}}\right)^2 \sum_{mnp=1}^N \int v_Y f_1[\omega, \mathbf{r}, \mathbf{v}] \sin\left(\frac{n\pi X'}{a}\right) \cos\left(\frac{m\pi Y'}{b}\right) \sin\left(\frac{p\pi z'}{d}\right) \\ & \quad \sin\left(\frac{n\pi X}{a}\right) \cos\left(\frac{m\pi Y}{b}\right) \sin\left(\frac{p\pi z}{d}\right) dX' dY' dz' d^3 v \\ & = \int K_Y^{(1)}(\mathbf{r}|\mathbf{r}') v_Y f_1[\omega, \mathbf{r}, \mathbf{v}] d^3 r' d^3 v \end{aligned}$$

where

$$K_Y^{(1)}(\mathbf{r}|\mathbf{r}') = \frac{\mu q (2\sqrt{2})^2}{abd} \sum_{mnp=1}^N \sin\left(\frac{n\pi X'}{a}\right) \cos\left(\frac{m\pi Y'}{b}\right) \sin\left(\frac{p\pi z'}{d}\right) \sin\left(\frac{n\pi X}{a}\right) \cos\left(\frac{m\pi Y}{b}\right) \sin\left(\frac{p\pi z}{d}\right) \quad (24)$$

Likewise

$$\frac{q}{\epsilon} \int f_{1,Y}[\omega, \mathbf{r}, \mathbf{v}] d^3 v = \int K_Y^{(2)}(\mathbf{r}|\mathbf{r}') f_1[\omega, \mathbf{r}, \mathbf{v}] d^3 r' d^3 v \quad (25)$$

where

$$\begin{aligned} K_Y^{(2)}(\mathbf{r}|\mathbf{r}') & = \frac{q(2\sqrt{2})^2}{\epsilon abd} \sum_{mnp=1}^N \left(\frac{-m\pi}{b}\right) \sin\left(\frac{n\pi X'}{a}\right) \sin\left(\frac{m\pi Y'}{b}\right) \\ & \quad \sin\left(\frac{p\pi z'}{d}\right) \sin\left(\frac{n\pi X}{a}\right) \cos\left(\frac{m\pi Y}{b}\right) \sin\left(\frac{p\pi z}{d}\right) \end{aligned} \quad (26)$$

$$E_Y(\mathbf{r}, \omega) = j\omega \int L_Y^{(1)}(\mathbf{r}|\mathbf{r}') v_Y f_1[\omega, \mathbf{r}, \mathbf{v}] d^3 r' d^3 v + \int L_Y^{(2)}(\mathbf{r}|\mathbf{r}') f_1[\omega, \mathbf{r}, \mathbf{v}] d^3 r' d^3 v \quad (27)$$

where

$$L_Y^{(1)}(\mathbf{r}|\mathbf{r}') = \frac{\mu q(2\sqrt{2})^2}{abd} \sum_{mnp=1}^N \sin\left(\frac{n\pi X'}{a}\right) \cos\left(\frac{m\pi Y'}{b}\right) \sin\left(\frac{p\pi z'}{d}\right) \sin\left(\frac{n\pi X}{a}\right) \cos\left(\frac{m\pi Y}{b}\right) \sin\left(\frac{p\pi z}{d}\right) \\ \frac{1}{\left(k^2 - \left(\frac{n^2}{a^2} + \frac{m^2}{b^2} + \frac{p^2}{d^2}\right) \pi^2\right)} \quad (28)$$

and

$$L_Y^{(2)}(\mathbf{r}|\mathbf{r}') = \frac{q(2\sqrt{2})^2}{\epsilon abd} \sum_{mnp=1}^N \left(\frac{-m\pi}{b}\right) \sin\left(\frac{n\pi X'}{a}\right) \sin\left(\frac{m\pi Y'}{b}\right) \sin\left(\frac{p\pi z'}{d}\right) \sin\left(\frac{n\pi X}{a}\right) \cos\left(\frac{m\pi Y}{b}\right) \sin\left(\frac{p\pi z}{d}\right) \\ \frac{1}{\left(k^2 - \left(\frac{n^2}{a^2} + \frac{m^2}{b^2} + \frac{p^2}{d^2}\right) \pi^2\right)} \quad (29)$$

Finally

$$E_z(\mathbf{r}, \omega) = j\omega \int L_z^{(1)}(\mathbf{r}|\mathbf{r}') v_z f_1[\omega, \mathbf{r}, \mathbf{v}] d^3 r' d^3 v + \int L_z^{(2)}(\mathbf{r}|\mathbf{r}') f_1[\omega, \mathbf{r}, \mathbf{v}] d^3 r' d^3 v \quad (30)$$

where

$$L_z^{(1)}(\mathbf{r}|\mathbf{r}') = \frac{\mu q(2\sqrt{2})^2}{abd} \sum_{mnp=1}^N \sin\left(\frac{n\pi X'}{a}\right) \sin\left(\frac{m\pi Y'}{b}\right) \cos\left(\frac{p\pi z'}{d}\right) \sin\left(\frac{n\pi X}{a}\right) \sin\left(\frac{m\pi Y}{b}\right) \cos\left(\frac{p\pi z}{d}\right) \\ \frac{1}{\left(k^2 - \left(\frac{n^2}{a^2} + \frac{m^2}{b^2} + \frac{p^2}{d^2}\right) \pi^2\right)} \quad (31)$$

and

$$L_z^{(2)}(\mathbf{r}|\mathbf{r}') = \frac{q(2\sqrt{2})^2}{\epsilon abd} \sum_{mnp=1}^N \left(\frac{-p\pi}{d}\right) \sin\left(\frac{n\pi X'}{a}\right) \sin\left(\frac{m\pi Y'}{b}\right) \sin\left(\frac{p\pi z'}{d}\right) \sin\left(\frac{n\pi X}{a}\right) \sin\left(\frac{m\pi Y}{b}\right) \cos\left(\frac{p\pi z}{d}\right) \\ \frac{1}{\left(k^2 - \left(\frac{n^2}{a^2} + \frac{m^2}{b^2} + \frac{p^2}{d^2}\right) \pi^2\right)} \quad (32)$$

So our first order Boltzmann equation becomes

$$j\omega f_1(\mathbf{r}, \omega, \mathbf{v}) + (\mathbf{v}, \nabla_{\mathbf{r}}) f_1(\mathbf{r}, \omega, \mathbf{v}) - \beta q(\mathbf{E}(\mathbf{r}, \omega), \mathbf{v}) f_0(\mathbf{r}, \omega) + \frac{f_1(\mathbf{r}, \omega, \mathbf{v})}{\tau} = 0 \quad (33)$$

where

$$(\mathbf{E}(\mathbf{r}, \omega), \mathbf{v}) = j\omega \sum_{k=1}^3 v_k \int L_K^{(1)}(\mathbf{r}|\mathbf{r}') v'_k f_1[\omega, \mathbf{r}, \mathbf{v}'] d^3 r' d^3 v' + \sum_{k=1}^3 v_k \int L_K^{(2)}(\mathbf{r}|\mathbf{r}') f_1[\omega, \mathbf{r}, \mathbf{v}'] d^3 r' d^3 v' \\ = j\omega \int L^{(1)}(\mathbf{r}, \mathbf{v}|\mathbf{r}', \mathbf{v}') f_1[\omega, \mathbf{r}', \mathbf{v}'] d^3 r' d^3 v' + \int L^{(2)}(\mathbf{r}, \mathbf{v}|\mathbf{r}', \mathbf{v}') f_1[\omega, \mathbf{r}', \mathbf{v}'] d^3 r' d^3 v' \quad (34)$$

where

$$L^{(1)}(\mathbf{r}, \mathbf{v}|\mathbf{r}', \mathbf{v}') = \sum_{k=1}^3 v_k v'_k L_K^{(1)}(\mathbf{r}|\mathbf{r}') \quad (35)$$

and

$$L^{(2)}(\mathbf{r}, \mathbf{v}|\mathbf{r}', \mathbf{v}') = \sum_{k=1}^3 v_k v'_k L_K^{(2)}(\mathbf{r}|\mathbf{r}') \quad (36)$$

Then

$$\left[j\omega + (\mathbf{v}, \nabla_r) - \beta q(j\omega\beta L^{(1)} + \beta L^{(2)}) + \frac{1}{\tau} \right] f_1 = 0 \quad (37)$$

from which after discretization the eigenfrequencies can be determined as from the root of

$$\det \left[j\omega + (\mathbf{v}, \nabla_r) - \beta q(j\omega\beta L^{(1)} + \beta L^{(2)}) + \frac{1}{\tau} \right] = 0 \quad (38)$$

4. RESULTS AND DISCUSSION

In multilinear algebra tensor decomposition is accomplished by projecting the space to lower dimensional representations. A tensor subspace is translated by a multilinear projection that maps the input data from a high-dimensional space to a low-dimensional space. Multilinear projection from a tensor space to a vector space is known as the tensor-to-vector projection (TVP). As a vector can be considered as multiple scalars, the projection from a tensor to a vector can be regarded as multiple projections, each of which projects a tensor to a scalar.

Discretization of Equation (37) is done as follows. Let us consider
 $k = \sqrt{\mu\epsilon\omega^2}$; $T = 300$ kelvin; $\tau = 2.5 \times 10^{-9}$ sec; $\beta = \frac{1}{T \times 1.38 \times 10^{-23}}$;
 $N = 2$; $a = 0.02$ m; $b = 0.01$ m; $d = 0.005$ m;
 $n_e = 10^{-16}$; $q = n_e * 1.6 \times 10^{-19} * a * b * d$ coul;
 $\Delta_x = \frac{a}{N}$, $\Delta_y = \frac{b}{N}$, $\Delta_z = \frac{d}{N}$; $v_{x(\max)} = 400$; $v_{y(\max)} = 400$; $v_{z(\max)} = 400$;
 $\delta_x = \frac{v_{x(\max)}}{N}$, $\delta_y = \frac{v_{y(\max)}}{N}$, $\delta_z = \frac{v_{z(\max)}}{N}$;
 $X = n_x \Delta_x$; $Y = n_y \Delta_y$; $z = n_z \Delta_z$; $\dot{X} = \dot{n}_x \Delta_x$, $\dot{Y} = \dot{n}_y \Delta_y$, $\dot{z} = \dot{n}_z \Delta_z$;
 $v_x = m_x \delta_x$, $v_y = m_y \delta_y$, $v_z = m_z \delta_z$; $\dot{v}_x = \dot{m}_x \delta_x$, $\dot{v}_y = \dot{m}_y \delta_y$, $\dot{v}_z = \dot{m}_z \delta_z$;
and $1 \leq (m_x, m_y, m_z, n_x, n_y, n_z) \leq N$.

Substituting the above values in Equations (21), (22), (28), (29), (31), and (32), then we will compute Equations (35) and (36). Let us consider discrete function \underline{f}_1 to be

$$\underline{f}_1 = \sum_{\underline{n}, \underline{m}}^{e(n)} f_1(\underline{n}, \underline{m}) (e(\underline{n}) \otimes e(\underline{m}))$$

We used matlab programming tool, in which we assume $A = eye(N)$ and $e(n_x) = A(:, n_x)$
 \otimes denotes the outer product.

$$\underline{f}_1 = \sum_{\underline{n}, \underline{m}}^{e(n)} f_1(\underline{n}, \underline{m}) e(n_x) \otimes e(n_y) \otimes e(n_z) \otimes e(m_x) \otimes e(m_y) \otimes e(m_z) \quad (39)$$

Then $e(n_x) \otimes e(n_y) = A(:, n_x) * transpose(A(:, n_y))$

$$f_1(\underline{n}, \underline{m}) = [e(n_x)^T \otimes e(n_y)^T \otimes e(n_z)^T \otimes e(m_x)^T \otimes e(m_y)^T \otimes e(m_z)^T] \underline{f}_1 \quad (40)$$

The second term of Equation (38) is given by

$$\begin{aligned} \mathbf{v}, \nabla_r = & \sum_{\underline{n}, \underline{m}}^{e(n)} \left(\frac{m_x \delta_x}{\Delta_x} ((e(n_x + 1)^T - e(n_x)^T) \otimes e(n_y)^T \otimes e(n_z)^T \otimes e(\underline{m})^T) \right. \\ & + \frac{m_y \delta_y}{\Delta_y} (e(n_x)^T \otimes (e(n_y + 1)^T - e(n_y)^T) \otimes e(n_z)^T \otimes e(\underline{m})^T) \\ & \left. + \frac{m_z \delta_z}{\Delta_z} (e(n_x)^T \otimes e(n_y)^T \otimes (e(n_z + 1)^T - e(n_z)^T) \otimes e(\underline{m})^T) \right) \end{aligned}$$

Eventually, we are able to evaluate the determinant of Equation (38). We can view determinant as a function in which input is a square matrix, and its output is a number. In present situation, the determinant of Equation (38) signifies the volume scaling factor of an n dimensional cube spanned by

its row and column vectors. This means that the matrix on the left side of equality in Equation (38) maps the unit n -cube to the n -dimensional space defined by the vectors. Hypercube or n -cube is a higher dimension analogous extension of a cube.

For a continuous function, there are infinite number of Green’s functions and eigenfunctions, which after discretization necessarily limits the eigenfunction and leads to gauging the values of eigenfrequencies by a suitable mathematical numerical method. As in continuous function, it is not feasible to represent all possible solutions in computer due to the finite nature of calculation method. Discretization provides a reasonable number of base functions within the simulation domain to acquire an approximate solution.

For the convenience of representation, let us assume the determinant of Equation (38) as \mathcal{A} . Now turn tensor \mathcal{A} into a matrix A . Through well established matrix computations, we discover things about A and draw conclusions about tensor \mathcal{A} based on what is learned about matrix A . Tensor unfoldings of $\mathcal{A} \in \mathfrak{R}^{N \times N \times N \times N \times N \times N}$ are carried out. There are many ways to assemble derived tensor \mathcal{A} entries into a matrix A that could be a block matrix whose entries are A -slices. A slice of a tensor \mathcal{A} is a matrix obtained by fixing all but two of \mathcal{A} ’s indices. We adopt the convention that the first unfixed index in the tensor is the row index of the slice, and the second unfixed index in the tensor is the column index of the slice. A fiber of a tensor is a column vector defined by fixing all but one index and varying the rest. A mode- k unfolding of a tensor is obtained by assembling all the mode- k fibers into a matrix. The matlab tensor toolbar function “tenmat” can be used to produce modal unfoldings.

If $\mathcal{A} \in \mathfrak{R}^{n_1 \times \dots \times n_d}$, $N = n_1 \dots n_d$ $B = \text{tenmat}(A, k)$ gives the mode- k unfolding, then B is the matrix $\mathcal{A}_{(k)} \in \mathfrak{R}^{n_k \times (N/n_k)}$ with

$$\mathcal{A}_{(k)}(i_k, \text{col}(\tilde{\mathbf{i}}_k, \tilde{\mathbf{n}})) = \mathcal{A}(\mathbf{i})$$

where

$$\begin{aligned} \tilde{\mathbf{i}}_k &= [i_1, \dots, i_{k-1}, i_{k+1}, \dots, i_d] \\ \tilde{\mathbf{n}} &= [n_1, \dots, n_{k-1}, n_{k+1}, \dots, n_d] \end{aligned}$$

Here col function maps multi-indices to integers. This precisely shows the order in which fibers are assembled.

For the present case, we need to solve the determinant, hence we flatten the tensor into a block matrix to get a square matrix. Block matrix is a matrix whose entries are matrices. Here $\mathcal{A} \in \mathfrak{R}^{n_1 \times n_2 \times n_3 \times n_4 \times n_5 \times n_6}$, $\text{tenmat}(A, [3 \ 4 \ 5 \ 6], [1 \ 2])$ sets up

$$\begin{bmatrix} \mathcal{A}(:, :, 1, 1, 1, 1) & \mathcal{A}(:, :, 1, 1, 2, 1) & \dots & \mathcal{A}(:, :, 1, 1, n_5, n_6) \\ \vdots & \vdots & \ddots & \vdots \\ \mathcal{A}(:, :, n_3, n_4, 1, 1) & \dots & \dots & \mathcal{A}(:, :, n_3, n_4, n_5, n_6) \end{bmatrix}$$

Table 1. Oscillation frequency of plasma filled rectangular cavity resonator.

Iteration (N)	Oscillation frequency (Hz)					
	Mode 1	Mode 2	Mode 3	Mode 4	Mode 5	Mode 6
$N = 2$	4.3288×10^9	2.6020×10^{10}	9.7166×10^{11}	1.1068×10^{12}	6.95×10^{12}	2.4010×10^{14}
$N = 3$	4.3601×10^9	2.7313×10^{10}	9.8050×10^{11}	1.1109×10^{12}	6.97×10^{12}	2.5202×10^{14}
$N = 4$	4.501×10^9	2.7316×10^{10}	9.8100×10^{11}	1.1109×10^{12}	7.00×10^{12}	2.5211×10^{14}

Table 1 shows the calculated frequency of oscillation. As we increase the number of iterations (N), oscillation frequency for that particular mode (m, n, p) approaches a fixed value. Fig. 1 indicates the graphical representation of resonant frequencies for ($N = 4$) for possible values of eigenmode, i.e., the value of (m, n, p).

4.1. Plasma Parameters

Plasma frequency is tuned by changing the plasma density and plasma conductivity such that it is possible for the same plasma antenna to resonate at different frequencies. Electronically, a smart plasma

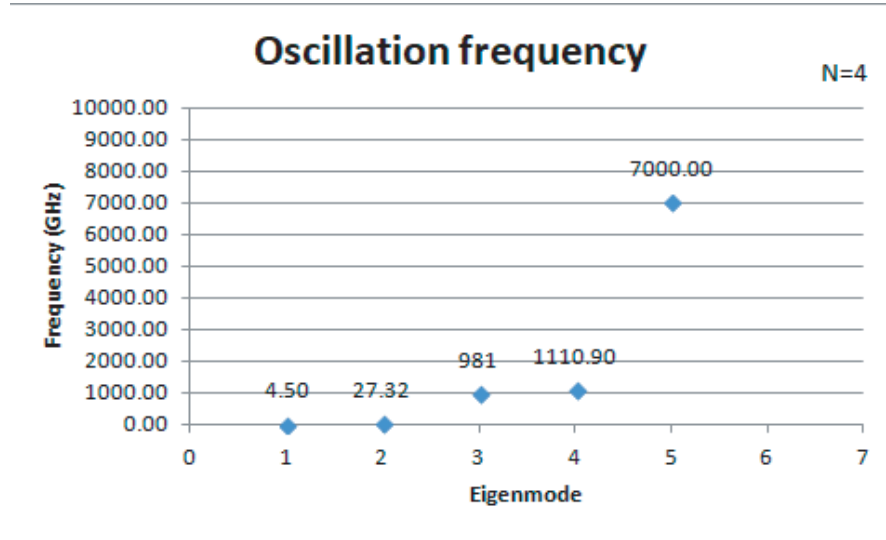


Figure 1. Oscillation frequencies for designated rectangular dielectric plasma filled cavity resonator.

antenna can steer the radiation pattern in different directions as in array antennas. Hence for these advantages, plasma antenna becomes an interesting and commendable research topic. Most of the work in literature on plasma antennas lacks the discussion about the dependency of resonance frequency and radiation pattern on antenna dimension and mainly deals with experimental approach. All the antenna parameters of the plasma antenna using High Frequency Structure Simulator (HFSS) are studied to understand the relation between resonance frequencies antenna dimension and plasma properties.

We can add parameters to DC generated plasma as we know voltage across plasma and current flowing through the plasma. However, it is difficult to add parameters for microwave generated plasma as the extent of ionization of gas is dependent on the operating microwave frequencies of microwave source. Parameters in HFSS could be added only if the ionization curves are known for plasma at different microwave frequencies.

Plasma conductivity with the collision frequency higher than the wave frequency ($\nu_m \gg \omega$) for the weakly ionized plasma can be calculated by the formula written below

$$\sigma = \frac{e^2 n_e}{m_e \nu_m}$$

Here e is the electronic charge, n_e the electron density, m_e the mass of electron, and ν_m the collision frequency.

Plasma is a material with electromagnetic properties as a nonhomogeneous, nonlinear, and dispersive medium, which makes plasma a special medium in which permeability (μ), conductivity (σ), and permittivity (ϵ) are a function of frequency and other parameters. For weakly ionized plasma, the external force on electron is assumed to be small, so that electron non-equilibrium distribution state is only slightly perturbed from its equilibrium position. The distribution function of electron is assumed to be inhomogeneous and anisotropic while distribution function of neutral particles of plasma is assumed as homogeneous and isotropic. A specific response results from any particular frequency of the excitation of electromagnetic wave and any particular density of ionization. Plasma partially absorbs radiated electromagnetic waves. Some EM waves are scattered, and some pass through the plasma. By appropriate selection of the basic parameters of plasma such as electron density and collision frequency, we can regulate the amount of EM wave to absorb, scatter, or pass through the plasma medium. The relative permittivity of plasma is calculated by the formula

$$\epsilon_r = \epsilon'_r - j\epsilon''_r = 1 - \frac{\omega_p^2}{\omega(\omega - j\nu_m)}$$

where ω_p is the plasma frequency, ω the operating frequency, and ν_m the collision frequency. Plasma frequency depends on the amount of ionization in the plasma and is characterized by the minimum

frequency of electromagnetic wave which can travel through that plasma specimen without attenuation. Plasma frequency is distinguished by the operating frequency of the plasma antenna, where operating frequency is equivalent to the operating frequency of a metal antenna of same dimension. Plasma frequency is equal to

$$\omega_p = \sqrt{\frac{4\pi n_e e^2}{m_e}}$$

4.2. Simulations

We first define plasma material to design a plasma antenna on HFSS which requires to define plasma conductivity, permittivity, and plasma density. They are calculated theoretically. For present plasma antenna model, the electron density is taken to be $n_e \sim 10^{-16} \text{ m}^{-3}$ and the collision frequency picked as $\nu_m \sim 4 \times 10^8 \text{ Hz}$. However, it is assumed that collision between particles does not affect plasma density and hence its distribution function. If this condition is met, we can apply collisionless Boltzmann equation for plasma. The plasma conductivity turns out to be $\sigma = 22 \text{ simens/m}^3$, and the plasma frequency is calculated to $\omega_p = 30 \times 10^6 \text{ Hz}$.

4.3. Design of Antenna

A model based on (high frequency simulation software) HFSS of plasma antenna can be simulated with mentioned values. Fig. 2 indicates schematic of a plasma antenna under consideration. Fig. 3 shows its side view. The configuration of designed plasma antenna consists of a glass box of dimension with *length* \times *width* \times *height* as $a = 20 \text{ mm}$, $b = 10 \text{ mm}$, $d = 5 \text{ mm}$, respectively, having 0.1 mm thickness. A plasma volume is grown inside the box.

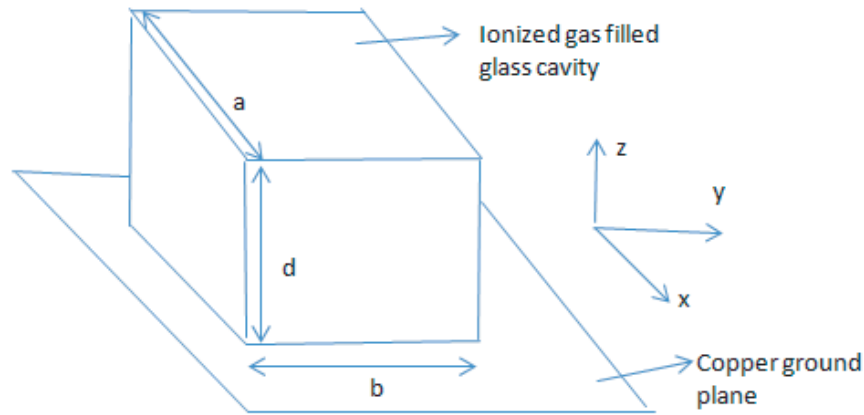


Figure 2. Dimension of designed rectangular dielectric resonator antenna.

For the present simulation of plasma antenna model, we assume the plasma density to be uniform. a copper plate of $100 \text{ mm} \times 100 \text{ mm}$ in x - y plane and a thickness of 0.1 mm is considered as ground plane. An air volume box is designated as a radiation boundary to set up for the far field pattern of the antenna. Between the plasma volume and copper ground plane coaxial waveport is assigned with the help of a small gap. For odd mode excitation, an integration line of wave port is taken between two conductors. For even mode excitation, a waveport integration line is taken between a conductor and ground plane. Fig. 4 is the model of plasma antenna with assigned parameters designed on HFSS software. For the present case of simulation purpose we assume $(m, n, p) = (1, 1, 1)$ and at center frequency at 3 GHz with a frequency sweep between 1 GHz and 10 GHz.

Ionized gas in glass box behaves like plasma. At assumed operating frequency 3 GHz, permittivity is calculated. In the present case, the real part of permittivity is approximately equal to one, and imaginary part of permittivity is much less than one, which results in dielectric loss tangent around

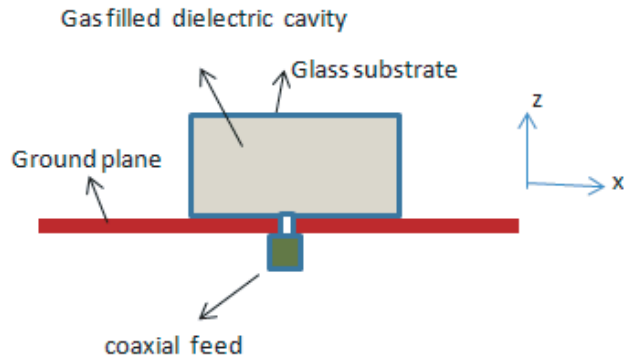


Figure 3. Side view of designed rectangular dielectric resonator antenna.

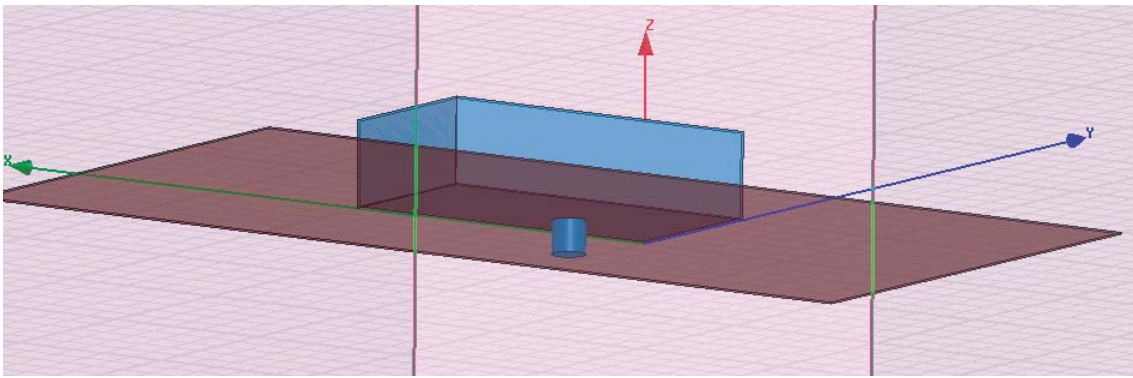


Figure 4. Simulated design of plasma filled rectangular dielectric resonator antenna.

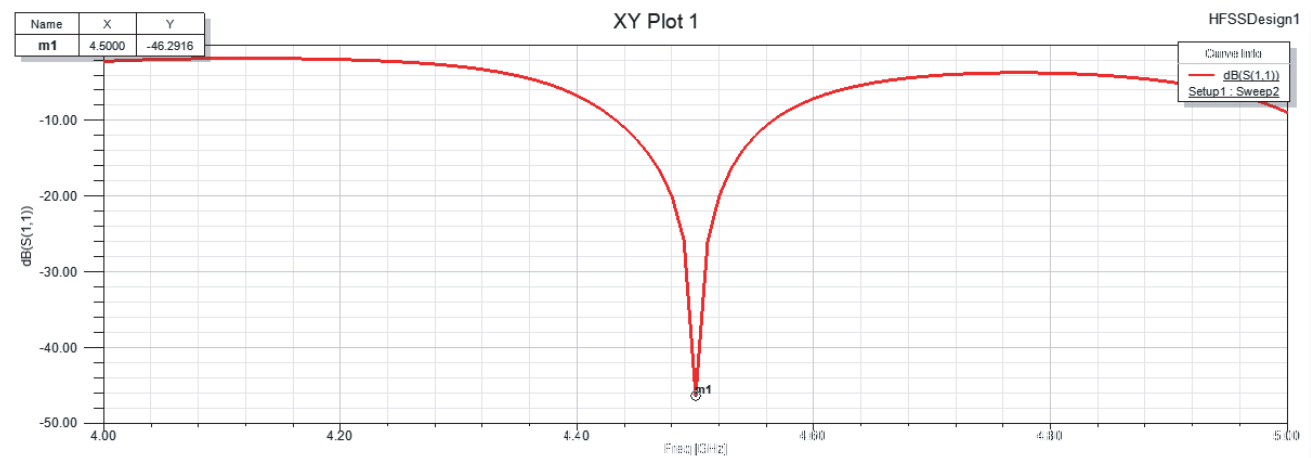


Figure 5. Return loss (S_{11}) parameter of simulated model of plasma filled rectangular dielectric resonator antenna.

zero. For different operating permittivity changes, plasma material is assigned by setting described parameter in HFSS. Fig. 5 shows the return loss (S_{11}) parameter of simulated model of the plasma filled rectangular dielectric resonator antenna. The more negative the value of return loss is, the higher the antenna gain is. As can be noticed in Fig. 5, return loss is -46 dB, at 4.5 GHz, which signifies that the designed model works very efficiently as an antenna (transmitter or receiver) at 4.5 GHz.

5. CONCLUSION

A generalized mathematical analysis for the computation of oscillation frequency for a plasma filled cavity resonator is accomplished. We employ a numerical perturbation method for solving governing Maxwell equation which resorts to appropriate boundary condition for rectangular cavity. We compare the results calculated by matlab and HFSS simulation for a specific configuration of designed plasma antenna. Resulting oscillation frequencies by the two simulation methods match reasonably well, which substantiate the exercise of perturbation method for estimating resonant frequency for a plasma filled cavity resonator.

ACKNOWLEDGMENT

The authors are thankful for support and worthwhile advice to colleagues and seniors during this work. Their criticisms and contributions are of outmost importance. I am feeling contented in presenting this research work. This piece of research work take its shape by valuable guidance of my research supervisors.

APPENDIX A. MULTILINEAR SUBSPACE ALGEBRA

The d th order tensor resides in the tensor space $\mathfrak{R}^{I_1} \otimes \mathfrak{R}^{I_2} \otimes \dots \otimes \mathfrak{R}^{I_d}$, where \mathfrak{R}^{I_d} is the n th vector space. Let \mathcal{A} be a d^{th} order tensor, which can be decomposed as follows.

$$\mathcal{A} = S \otimes u_1 \otimes u_2 \otimes \dots \otimes u_d \quad (\text{A1})$$

where \otimes stands for outer product (tensor product). The outer product operation is a way of combining an order- d_1 tensor and an order- d_2 tensor to obtain an order- $(d_1 + d_2)$ tensor. S is the core matrix, whose outer product is taken with $d = 1 \dots N$ matrices. u_d is the $I_d \times I_d$ matrix with orthogonal column vector.

To find the projection of tensor \mathcal{A} defined in a tensor space $\mathfrak{R}^{I_1} \otimes \mathfrak{R}^{I_2} \otimes \dots \otimes \mathfrak{R}^{I_d}$ to another lower dimensional tensor space defined by matrix S is given by

$$S = \mathcal{A} \otimes u_1^T \otimes u_2^T \otimes \dots \otimes u_d^T \quad (\text{A2})$$

We can also write decomposition as

$$\mathcal{A} = \sum_{i_1}^{i_d} S(i_1, i_2 \dots i_d) \otimes u_1 \otimes u_2 \otimes \dots \otimes u_d$$

which indicates that any tensor, for example \mathcal{A} , can be expressed as a linear combination of rank one tensors.

$$\prod_{N=1}^{d=1} I_d$$

A Tucker product representation where the inverse factor matrices are the left singular vector matrices for the unfoldings $\mathcal{A}_{(1)}, \dots, \mathcal{A}_{(d)}$.

REFERENCES

1. Erden, F., "Evolutionary approach to solve an novel time-domain cavity problem," *Journal of Latex Class Files*, Vol. 14, No. 8, August 2015.
2. Yaduvanshi, R. S. and H. Parthasarathy, *Rectangular Dielectric Resonator Antennas: Theory and Design*, Springer, September 2015.
3. Epstein, I. L. and M. Gavrilovic, "The study of a homogeneous column of argon plasma at a pressure of 0.5 torr, generated by means of the Beenakker's cavity," *The European Physical Journal D*, 2014.
4. Moskvitina, Y. K. and G. I. Zaginaylova, "Effect of background plasma on electromagnetic properties of coaxial gyrotron cavity," *Technical Physics*, Vol. 59, No. 7, 1065–1071, 2014.

5. Liu, S., Z. He, S. Cheng, and S. Y. Zhong, "Symplectic finite-difference time-domain scheme based on decomposition technique of the exponential operator for plasma media," *IET Microwaves, Antennas and Propagation*, Vol. 10, No. 2, 129–133, 2016.
6. Yuan, J. and G. Lin, "Design of compact circular resonator for electrodeless microwave plasma lamp," *Electronics Letters*, Vol. 49, No. 16, August 2013.
7. Buchel, A., "Relaxation time of non-conformal plasma," *Physics Letters B*, 200–203, 2009.
8. Shuvalov, V. A. and A. I. Priimak, "A probe diagnostics for high-speed flows of rarefied partially dissociated plasma," *Instruments and Experimental Techniques*, Vol. 50, No. 3, 370–378, 2007.
9. Melrose, D. B., "Kinetic plasma physics," *Swiss Society for Astrophysics and Astronomy*, Vol. 24, 113–223, Springer, 1994.
10. Marsch, E., "Kinetic physics of the solar wind plasma," *Physics and Chemistry in Space — Space and Solar Physics*, Vol. 21, 1991.
11. Xiao, S. and Y. L. Mo, "Study of open cavity filled with plasma density grating," *IEEE Transactions on Plasma Science*, Vol. 27, No. 5, 1495–1500, October 1999.
12. Oleinik, A. M., "Dwell time in the excitation zone for particles blown into the plasma of a spark discharge," 224–225, Consultants Bureau, a division of Plenum Publishing Corporation, 227 West 7th Street, New York, N. Y. 10011, 1972.
13. Yakimenko, I. P. and T. R. Kelner, "The natural frequencies of cylindrical cavities with a magnetoactive plasma," *Radiophysics and Quantum Electronics*, Vol. 10, No. 6, 815–824, 1967.
14. Safari, S. and B. Jazi, "The plasma background effect on time growth rate of terahertz hybrid modes in an elliptical metallic waveguide with two electron beams as energy source," *IEEE Transactions on Plasma Science*, Vol. 44, No. 10, 2356–2365, October 2016.
15. Timofeev, A. V., "Time of relaxation in dusty plasma model," *Journal of Physics: Conference*, Series 653, 012137, 2015.
16. Singh, S. and M. V. Kartikeyan, "Full wave analysis of plasma loaded coaxial gyrotron cavity with triangular corrugations on the insert," *IEEE Transactions on Electron Devices*, Vol. 64, No. 5, 2369–2375, 2017.
17. Singh, S. and M. V. Kartikeyan, "Analysis of plasma loaded conventional and coaxial cavity with wedge-shaped corrugations on the insert," *IEEE Transactions on Electron Devices*, Vol. 65, No. 6, 2614–2619, 2018.
18. Bittencourt, J. A., *Fundamentals of Plasma Physics*, 3rd Edition, Springer International Addition, 2003.
19. Balanis, C. A., *Antenna Theory: Analysis and Design*, 2nd Edition, Wile Edition, 1938.
20. Francis, F. C., *Introduction to Plasma Physics and Controlled Fusion*, 2nd Edition, Springer International Addition, 1974.
21. Podolsky, V. and A. Semnani, "Experimental and numerical studies of a tunable plasma antenna sustained by RF power," *IEEE Transactions on Plasma Science*, Vol. 48, No. 10, 3524–3534, Oct. 2020.
22. Kalynov, Y. K. and A. V. Savilov, "Competition of oscillations at different cyclotron harmonics in the subterahertz large-orbit gyrotron," *IEEE Transactions on Electron Devices*, Vol. 67, No. 9, 3795–3801, Sept. 2020.
23. Cohen, G. and M. Galperin, "Green's function methods for single molecule junctions," *AIP, The Journal of Chemical Physics*, Vol. 152, 090901, 2020.